ELSEVIER Nuclear Instruments and Methods in Physics Research A 421 (1999) 163–175

NUCLEAR INSTRUMENTS & METHODS IN PHYSICS RESEARCH Section A

Optimization of sample height in cylindrical geometry for gamma spectrometry measurements

M. Barrera*, I. Ramos-Lerate, R.A. Ligero, M. Casas-Ruiz

Departamento de Física Aplicada, Universidad de Cádiz, E-11510-Puerto Real, Spain

Received 3 June 1997; received in revised form 11 November 1997

Abstract

A model was developed to determine the optimum height in cylindrical geometry samples, to measure by gamma spectrometry a given fraction of the maximum number of possible detections. The method was applied to samples of water and seabed sediment of the Bay of Cádiz (Southwestern Spain). The influence of sample density was also studied. An important goal of this method is to avoid measuring the different efficiencies for multiple heights. The method was validated in the usual energy range for environmental samples (100–1700 keV).

Keywords: Gamma spectrometry; Cylindrical geometry samples

1. Introduction

The measurement of the radioactivity in environmental samples is generally a low-level counting technique, therefore it is important to minimize the radiation coming from outside, using an adequate shield, and to maximize the detections coming from the sample itself, using the most optimum geometry to increase the counting efficiency (high source volumes and short detector-source distances).

For sediment samples, it is usual to employ cylindrical geometry in short detector-samples distances. In such a geometry, and for a fixed diameter, the detection rate increases as the column height of sediment grows. However, a column "limit-height" is reached beyond which the improvement in detection rate is insignificant. The reasons for this are due to self-absorption and worsening geometry for extended column layers. Knowledge of such a limit height can suppose an important time-saver in sample gathering and preparation.

This paper presents a method that relates the number of detections, D, and the height of a cylindrical sample, h. It will be shown that the number of detections approaches a limit although $D(h)$ is an increasing function. So, for a given fraction of the number of maximum detections it is possible to determine the optimum height in the sample.

Although the method was developed to study column height in cylindrical geometry samples, it is applicable to other geometries, like the Marinelli beaker.

* Corresponding author. Tel.: + 34 56 470849; fax: + 34 56 470866; e-mail: mbarrera@galeon.uca.es.

0168-9002/99/$ – see front matter
PII: S0168-9002(98)01228-5

2. Theoretical basis

The fundamental hypothesis of the method is the homogeneization of the sample, including the radioisotopes in it. Consider a sample containing a specific radioisotope of activity A, with a characteristic gamma-ray yield Y, measured over a time t. Then the number of emissions N is

$$N = AYt. \tag{1}$$

Let ε be the efficiency of the sample–detector system. Then the number of detections, D, is

$$D = \varepsilon AYt \tag{2}$$

or

$$D = \varepsilon N. \tag{3}$$

Equivalently,

$$\varepsilon = \frac{D}{N}. \tag{4}$$

In our model, we calculate a theoretical total sample–detector efficiency ε_t by generating photons in a random point of the sample and simulating their possible trajectories and interactions with the sample and detector. If N photons are emitted over a time t, and D photons are detected, then the theoretical total efficiency ε_t is

$$\varepsilon_t = \frac{D}{N}. \tag{5}$$

In the Monte Carlo method [1], each point of the sample is equally probable, as well as every starting direction to the trajectory. For the kth generated "primary-decay" photon to escape the sample, it must travel a distance x_k inside the sample (Fig. 1). If μ_M is the sample attenuation coefficient for a considered energy, the probability that the photon goes through the sample without interaction is $e^{-\mu_M x_k}$. If the path intercepts the detector, the probability of photon–detector interaction is $1 - e^{-\mu_D w_k}$, where μ_D is the attenuation coefficient of the detector and w_k is the pathway of the photon inside the detector. So, the probability for the kth photon to be detected is

$$p_k = e^{-\mu_M x_k} \cdot (1 - e^{-\mu_D w_k}) \tag{6}$$

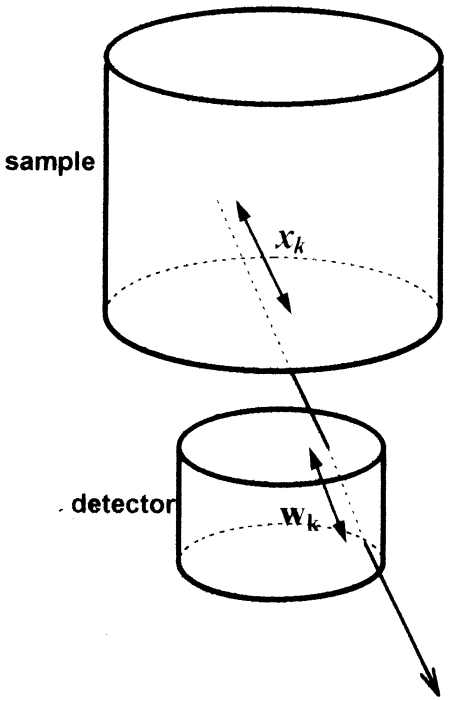

Fig. 1. Photon generation for a cylindrical geometry to be used in Monte Carlo method.

and, the total efficiency of the system for N generated photons inside the sample is

$$\varepsilon_t = \frac{D}{N} = \langle p_k \rangle = \frac{1}{N} \sum_{k=1}^{k=N} e^{-\mu_M x_k} \cdot (1 - e^{-\mu_D w_k}). \tag{7}$$

The attenuation correction in the path between sample and detector has not been considered because the photon attenuation coefficient for the air is thousand times less than the attenuation coefficient for the water or the sediment, so that the corrections would be less than the precision of our model, as we will show. The photon attenuation for the polyethylene cylindrical container and the window detector has either not been considered, because their thicknesses are negligible with respect to the dimensions of the sample and the detector.

A numerical model for calculating the photopeak efficiency would be much more complicated because there are multiple interactions contributing to the photopeak.

If we call the activity per volume unit a, then we can write Eq. (2) as

$$D = \varepsilon V a Y t, \tag{8}$$

where V is the sample volume. To simplify the analysis, we group the efficiency and volume terms into a single parameter β

$$\beta = \varepsilon V. \tag{9}$$

Now the number of detections can be written as

$$D = \beta a Y t. \tag{10}$$

We now concentrate all the geometrical dependence in the number of detections on β. Let h be the height of the cylindrical sample, and C a constant independent of system geometry, then while holding the cylinder radius constant,

$$D(h) = \beta(h) C, \tag{11}$$

β is an increasing function which has a finite value at infinite height $\beta(\infty)$, and is derived in the appendix. Beginning at $\beta(0) = 0$, the shape of the function β is the one represented in Fig. 2, analogous to the $D(h)$ shape except for a factor C.

To find a particular sample height h_Q that gives a fraction $Q(0 < Q < 1)$ of the maximum number of detections, $D(\infty)$, consists of resolving the equation:

$$D(h_Q) = Q D(\infty) \tag{12}$$

or the equivalent one:

$$\beta(h_Q) = Q \beta(\infty). \tag{13}$$

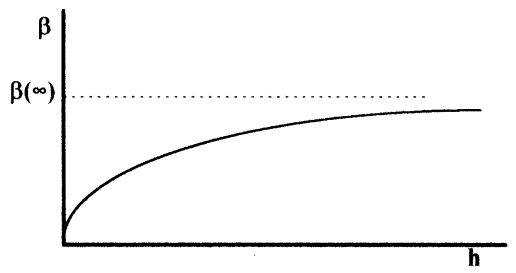

Fig. 2. β function shape.

It is known that for a given sample, the ratio between the photopeak efficiencies, ε, and the total efficiencies, ε_t, depends on the energy, E, and is nearly independent on the sample geometry and on the detector–sample relative position [2]. So:

$$\frac{\varepsilon(E, h)}{\varepsilon_t(E, h)} = r(E) \tag{14}$$

and considering the definition given in Eq. (9) we can write:

$$\beta(h) = r \cdot \beta_t(h) \tag{15}$$

which if it is replaced in Eq. (13), it leads to the equation:

$$\beta_t(h_Q) = Q \cdot \beta_t(\infty). \tag{16}$$

This equation needs to be solved the function $\beta_t(h)$, so we can get the total efficiency of the system using expression (7).

As we were interested in optimizing the height, not only for a unique value but for a range of energies, E_i, employ Eq. (16) for every one of these energies, obtaining the values $h_Q(E_i)$ corresponding to the values of an increasing function $h_Q(E)$.

3. Development of the method

We have applied the method to an integral preamplifier- CANBERRA GC2020-7500SL p-type coaxial HPGe detector system. The useful energy range of this detector is from 50 keV to more than 10 MeV. The Peak/Compton ratio is 46 for the 1333 keV ^{60}Co photon. The HPGe crystal is 50.5 mm in diameter and 46.5 mm in length. The relative efficiency to a 3 in × 3 in NaI(Tl) detector is 20% and the resolutions at 122 and 1332 keV of 1.1 and 2 keV, respectively. The detector–sample relative position is represented in Fig. 1. The sample–detector distance is 8 mm, the shortest in our case. The energy range we are interested is from 100 to 2000 keV.

We have developed a computer program that uses Eq. (7) in order to calculate the total efficiency corresponding to a given height of the sample, for

a set of energies E_j. So, if we consider n_h heights and n_E energies for every height, we get the matrix:

$$[\varepsilon_t(h_i, E_j)] = \begin{pmatrix} \varepsilon_t(h_1, E_1) & \varepsilon_t(h_2, E_1) & \dots & \varepsilon_t(h_{n_h}, E_1) \\ \varepsilon_t(h_1, E_2) & \varepsilon_t(h_2, E_2) & \dots & \varepsilon_t(h_{n_h}, E_2) \\ \dots & \dots & \dots & \dots \\ \varepsilon_t(h_1, E_{n_E}) & \varepsilon_t(h_2, E_{n_E}) & \dots & \varepsilon_t(h_{n_h}, E_{n_E}) \end{pmatrix} \quad (17)$$

which if multiplied by V_i gives:

$$[\beta_t(h_i, E_j)] = \begin{pmatrix} \beta_t(h_1, E_1) & \beta_t(h_2, E_1) & \dots & \beta_t(h_{n_h}, E_1) \\ \beta_t(h_1, E_2) & \beta_t(h_2, E_2) & \dots & \beta_t(h_{n_h}, E_2) \\ \dots & \dots & \dots & \dots \\ \beta_t(h_1, E_{n_E}) & \beta_t(h_2, E_{n_E}) & \dots & \beta_t(h_{n_h}, E_{n_E}) \end{pmatrix} \quad (18)$$

verifying for each element $\beta_t(h_i,E_j) = V_i \cdot \varepsilon_t(h_i, E_j) = \pi R_M^2 h_i \varepsilon_t(h_i, E_j)$, where R_M is the radius of the sample (in our case 32 mm).

We have chosen 11 or 13 energies, E_j, in which we know the attenuation of the sample, and we have taken 150 values for h_i inside the range from $h = 0$ to the finite value in which $\beta_t(\infty)$ is reached.

The statistical uncertainty has been fixed below 0.3%, which implies a calculation time of 24 h to determine the matrix $[\beta_t(h_i, E_j)]$.

4. Applications

4.1. Water sample

The optimization of the height has been made, firstly, for water samples. The attenuation coefficients for the water and the germanium have been taken from Ref. [3], and the energies we have used in our calculations are: 100, 150, 200, 300, 400, 500, 600, 800, 1000, 1500 and 2000 keV.

We have represented the values of β_t versus height for three energies in Figs. 3 and 4. Above 1000 mm the value $\beta_t(\infty)$ is essentially reached for all three energies (Fig. 4). $\beta_t(h)$ goes assymptotic to $\beta_t(\infty)$ as $h_i \to \infty$.

From the set of calculated points, we have fit β_t to a polynomial curve of sixth degree without

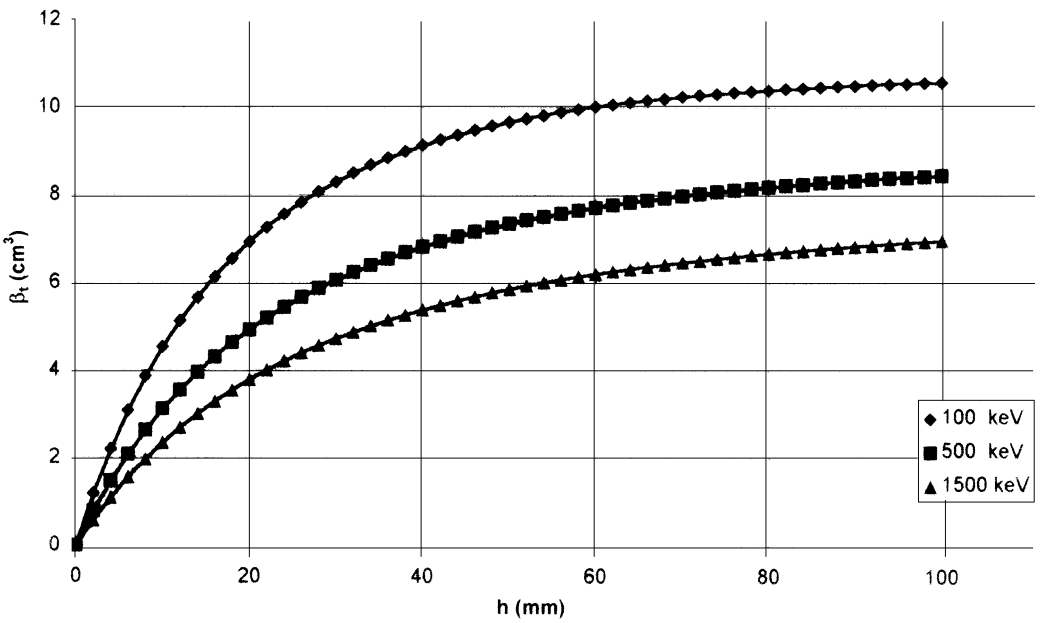

Fig. 3. β_t versus height, for three energies for a water sample.

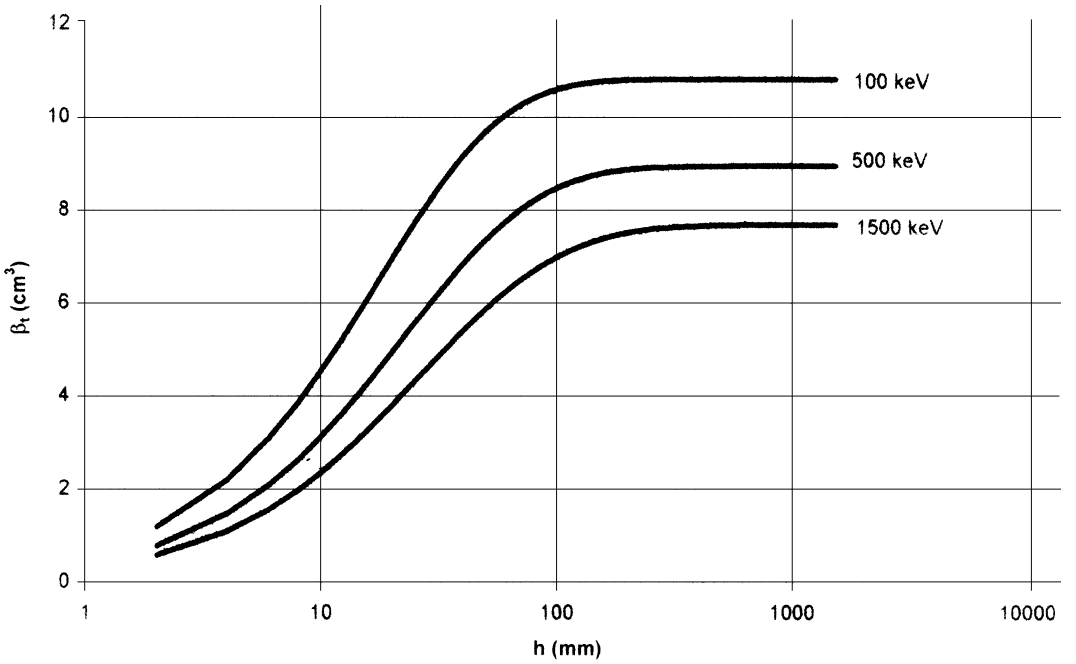

Fig. 4. β_t versus height, for three energies for a water sample, h is extended to show $\beta_t(\infty)$.

independent term, employing minimum square techniques

$$\beta_t(h, E_j) = \sum_{k=1}^{k=6} a_{kj} h^k. \tag{19}$$

Knowing this expression, it is possible to solve Eq. (16), to determine the height h_Q of the sample necessary to detect a fraction Q of the maximum number of detections.

We represent, in Fig. 5, the results obtained for desired detections fractions $Q = 0.75, 0.80$ and 0.85. For a given fraction Q the height h_Q increases with energy, and for a given energy, height h_Q increases with fraction Q.

Therefore, a water sample of height $h_Q = 50$ mm assures the percent of detections is above $Q = 75\%$ for all energies > 100 keV.

4.2. Sediment sample

The method has also been applied to a seabed sediment sample, after being dried, powdered, and less than 0.5 mm sieved in order to reach the homogeneity, whose attenuation coefficient was determined using the transmission method for the photons emitted by a point source of ^{152}Eu placed above the sample [4].

In Fig. 6, the values of β_t, obtained for 122, 867 and 1700 keV, are represented, and in Fig. 7, we extend the height range for checking how the values $\beta_t(\infty)$ are reached.

After the fit of β_t to a polynomial curve, Eq. (19), it is possible to solve Eq. (16) to optimize the height.

So, in Fig. 8, for each energy, we represent, the height values of sediment samples necessary to detect 75%, 80% and 85% of the maximum number of detections. We have to realize that the same percentage of detected emissions requires a lower height for the sediment sample than for the water sample, because of the lower attenuation in water.

4.3. Influence of density

Making environmental analysis by gamma spectrometry, samples of similar composition but different densities are often found [5]. So, they have the

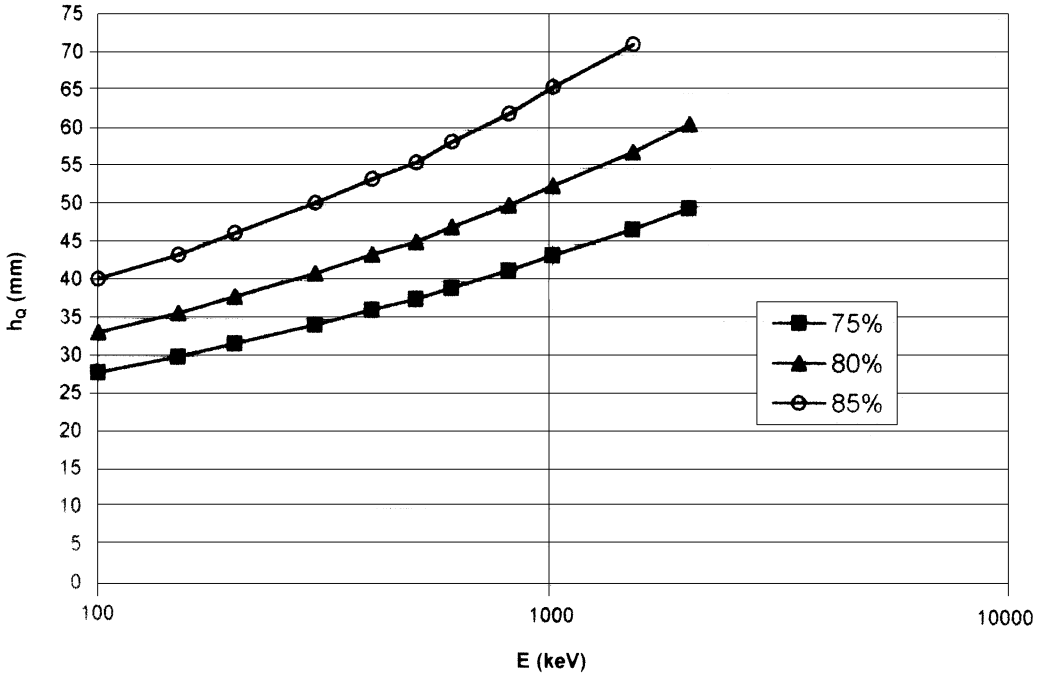

Fig. 5. h_Q versus energy, for a water sample and $Q = 0.75$, 0.80 and 0.85.

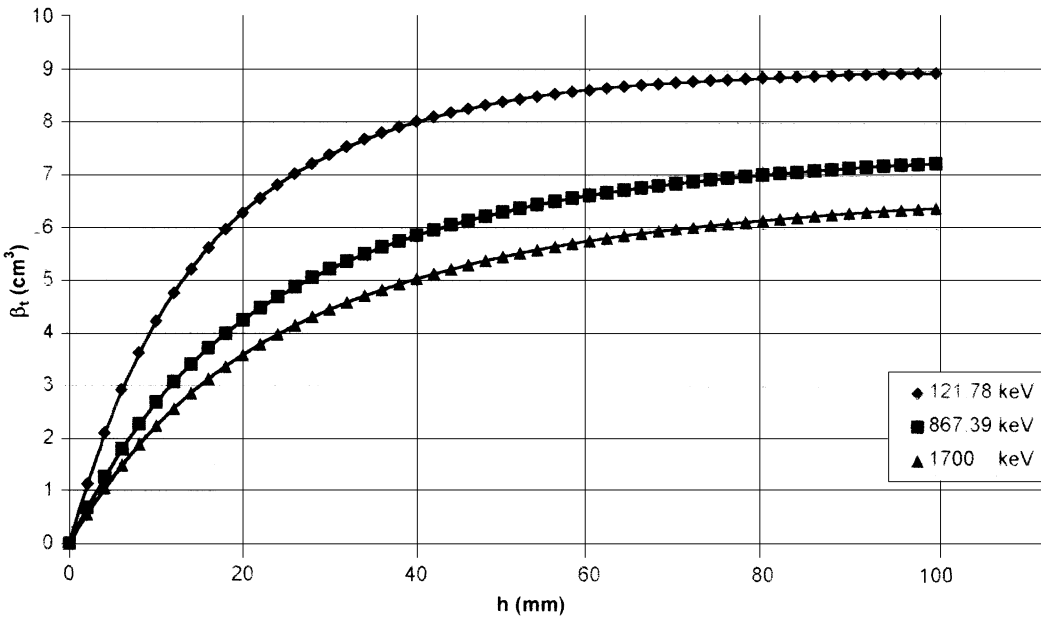

Fig. 6. β_t versus height, for three energies for a sediment sample.

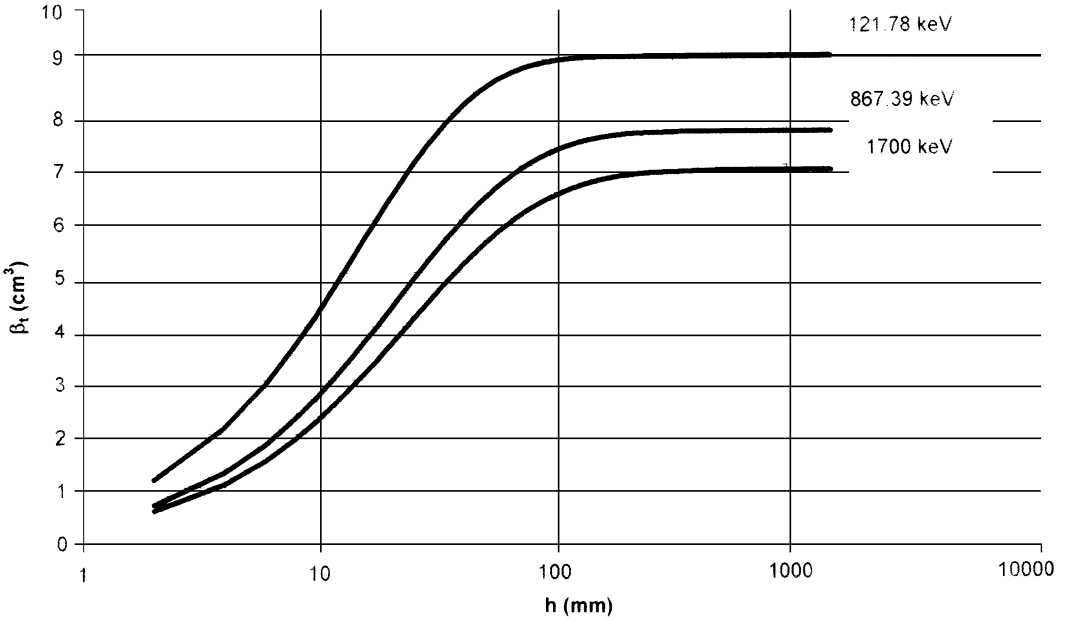

Fig. 7. β_t versus height, for three energies for a sediment sample, h is extended to show $\beta_t(\infty)$.

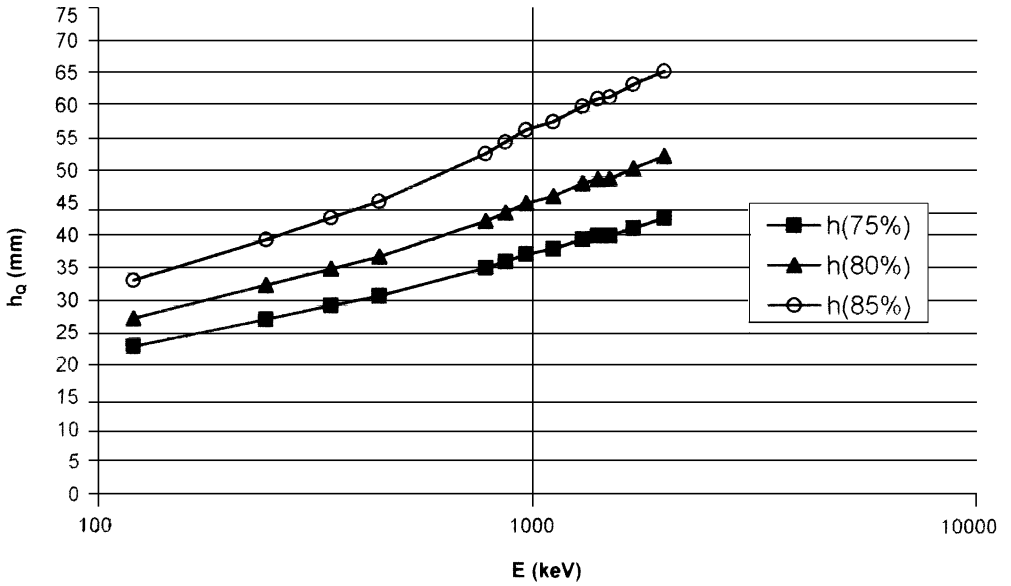

Fig. 8. h_Q versus energy, for a sediment sample and $Q = 0.75$, 0.80 and 0.85.

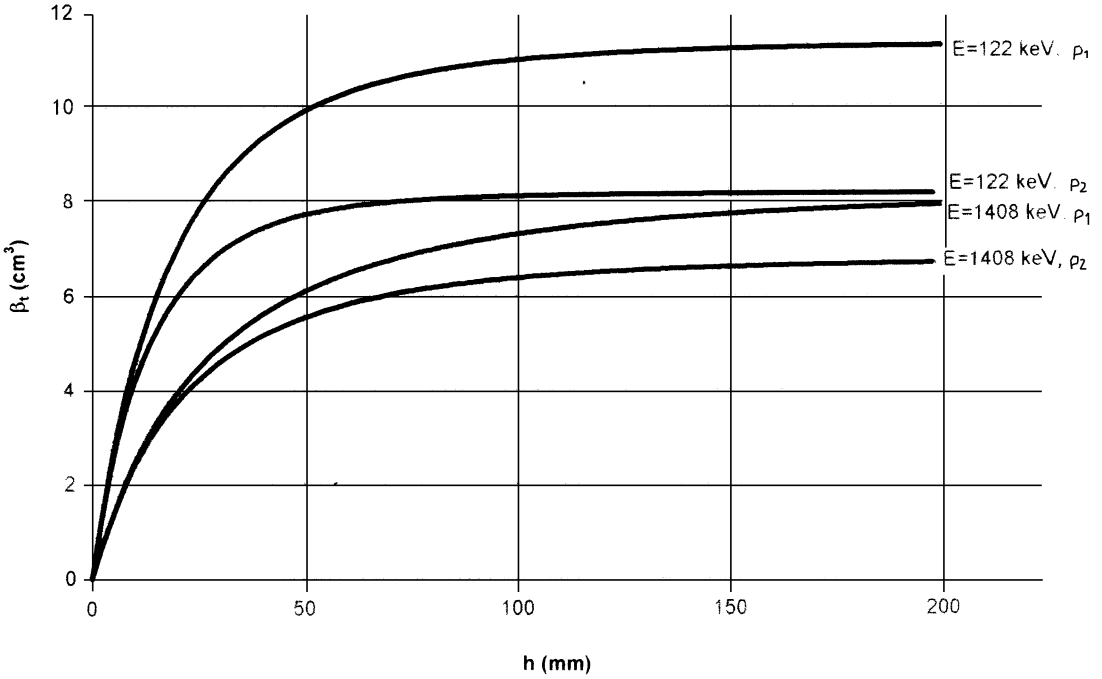

Fig. 9. β_t versus height, for two energies for sediment samples of density 1 and 2 g/cm^3.

same mass attenuation but a different linear attenuation. This happened with a set of seabed sediments of the Bay of Cádiz, whose densities varied between 1 and 2 g/cm^3. The lower-density samples have larger h_Q associated with a desired Q, as they have a lower linear attenuation.

In order to study this effect, the $\beta_t(h)$ curves are determined, for the densities $\rho_1 = 1$ g/cm^3 and $\rho_2 = 2$ g/cm^3. In Fig. 9, we have represented the results for energies 122 and 1408 keV and for a height range from 0 to 200 mm. We can observe, in this figure, how β_t, for every energy and height, is lower for the highest density, as a consequence of the bigger self-absorption. We can also see that when the limit value of $\beta_t(h)$ is reached for density ρ_2, the value of this function for ρ_1 still grows.

We can calculate the optimization height, for every energy and density, once we know the $\beta_t(h)$ curves. In Fig. 10 the obtained results are represented, for densities ρ_1 and ρ_2, corresponding to the fractions $Q = 0.75$ and $Q = 0.85$, and we can conclude that for a sample height of 55 mm, we detect more than 75% of the maximum number of detections, in all the sediments whose densities vary between 1 and 2 g/cm^3, and for the whole energy range we have considered.

5. Experimental validation

The photopeak detections in a sediment sample with different heights have been measured in order to validate the theoretical method that we have proposed.

The sediment used in the validation has a density of 1.64 g/cm^3 and has been injected with a mixed source, whose energies are: 88.03 keV (^{109}Cd), 122.06 keV (^{57}Co), 661.66 keV (^{137}Cs), 1173.24 and 1332.5 keV (^{60}Co), and 1461 keV (^{40}K). The former radioisotope does not belong to the mixed source, but appears like a natural emitter in the sediment.

The samples have been placed in 64 mm diameter polyethylene containers, which have been filled to 5, 10, 15 mm and so on to 70 mm height.

The mixed source has been homogenized in the sample, and such an homogenization has been

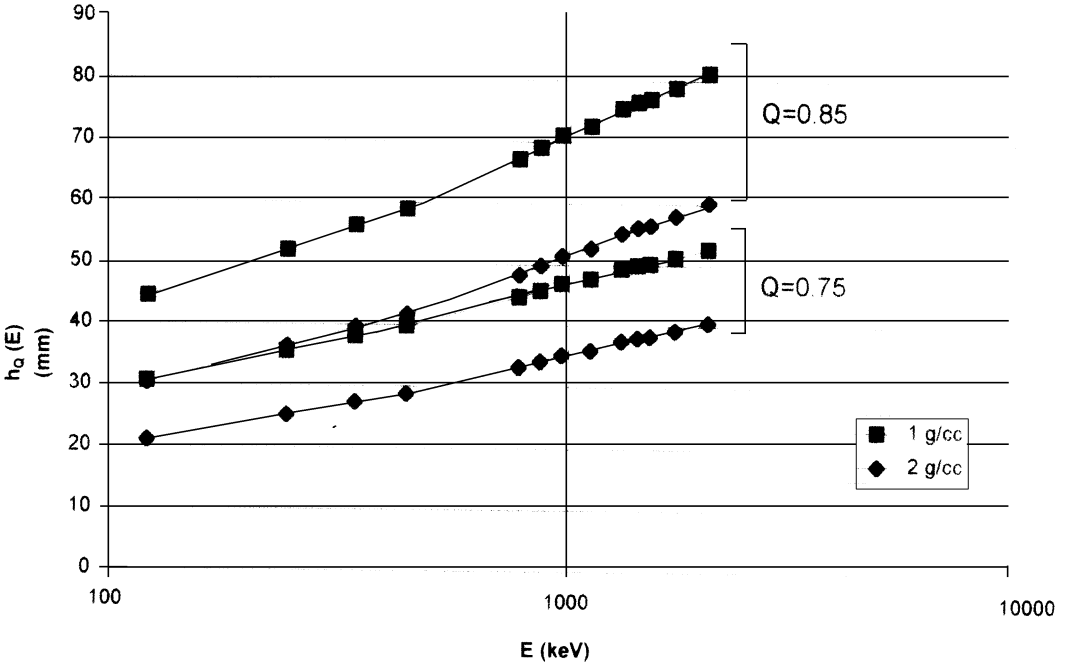

Fig. 10. h_Q versus energy, for sediment samples, of density 1 and 2 g/cm^3 and $Q = 0.75$ and 0.85.

verified making several measurements after mechanical shaking and checking that the number of the counts in every photopeak is constant, inside the statistical uncertainties [6].

From the values of the experimental photopeak efficiencies, for every energy and height, we can calculate the β_{exp} values, and we can fit these ones to a polynomial curve, Eq. (19).

In order to compare the results of the model and the experimental ones, we normalize the β functions to the values found for the maximum height ($h = 70$ mm). So, we calculate the ratios:

$$\frac{\beta_{exp}(h)}{\beta_{exp}(h_{max})} \quad \text{and} \quad \frac{\beta_t(h)}{\beta_t(h_{max})} \tag{20}$$

represented in Fig. 11, Fig. 12, and Fig. 13, for energies 662, 1173 and 1332 keV, where we have drawn the error bars in h and $\beta_{exp}(h)/\beta_{exp}(h_{max})$, although the latter are very small due to the good statistics in our measurements. We can observe here the agreement between the theoretical and the experimental results.

In our initial hypothesis (Eq. (14)), we established that the rate between the photopeak and total efficiencies depends on the energy and is approximately constant with respect to the height. This approximation can explain the slight and systematic deviation between both functions.

Nomenclature

a_{kj}	coefficient of β fit
A	sample activity
C	sample geometry independent constant
D	number of detections
D_0	distance from the sample-bottom to the detector-center
E	photon energy
h	sample height
h_{max}	maximum sample experimental height
h_Q	optimum sample height
n_E	number of energies for β calculation
n_h	number of heights for β calculation
N	number of emissions

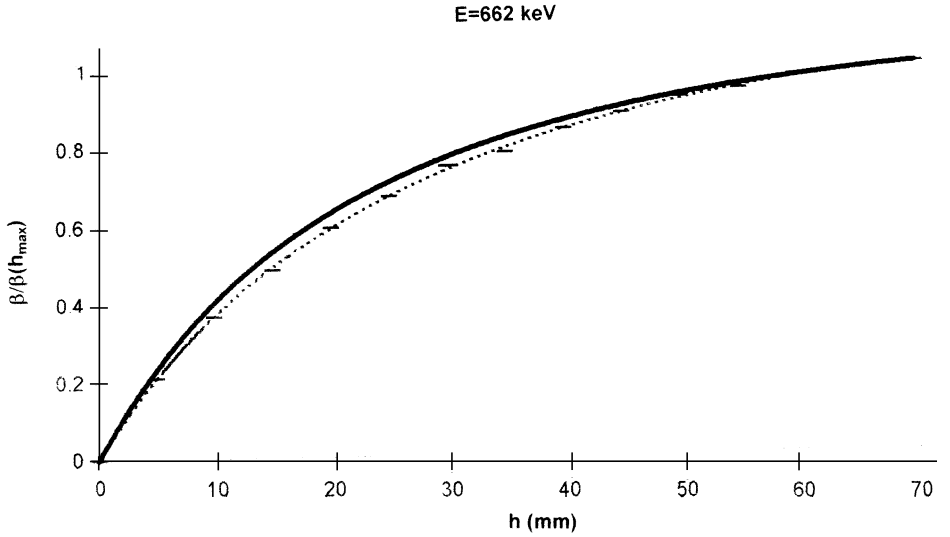

Fig. 11. Normalized β functions, theoretical and experimental, for 662 keV energy. The dot lines represent the experimental function.

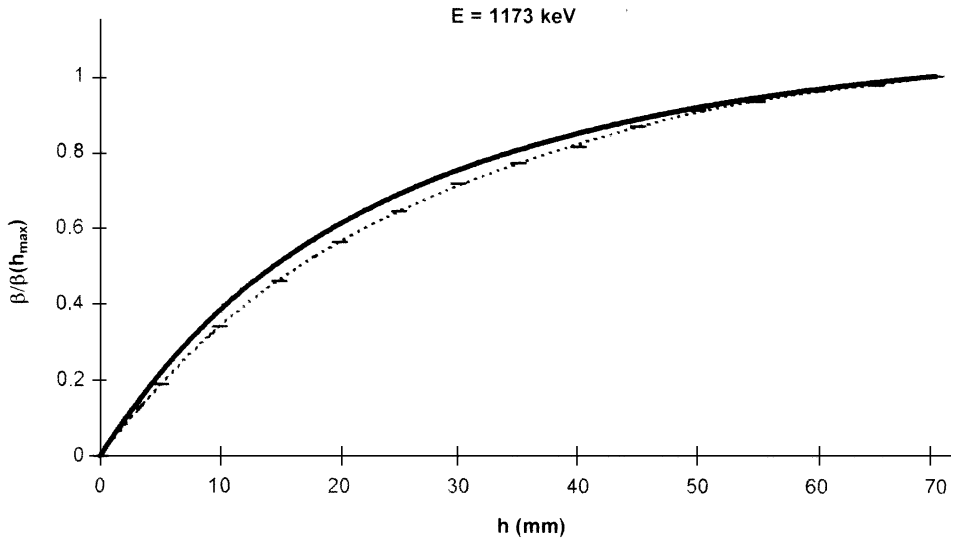

Fig. 12. Normalized β functions, theoretical and experimental, for 1173 keV energy. The dot lines represent the experimental function.

p_k probability for the photon to be detected
p_1 probability for the photon to be emitted toward the detector
p_2 probability for the photon not to be absorbed in the sample
p_3 probability for the photon to be detected when it crosses the detector
Q fraction of the maximum number of detections
R_D detector radius
R_M sample radius
r ratio between the photopeak and the total efficiencies
t counting time

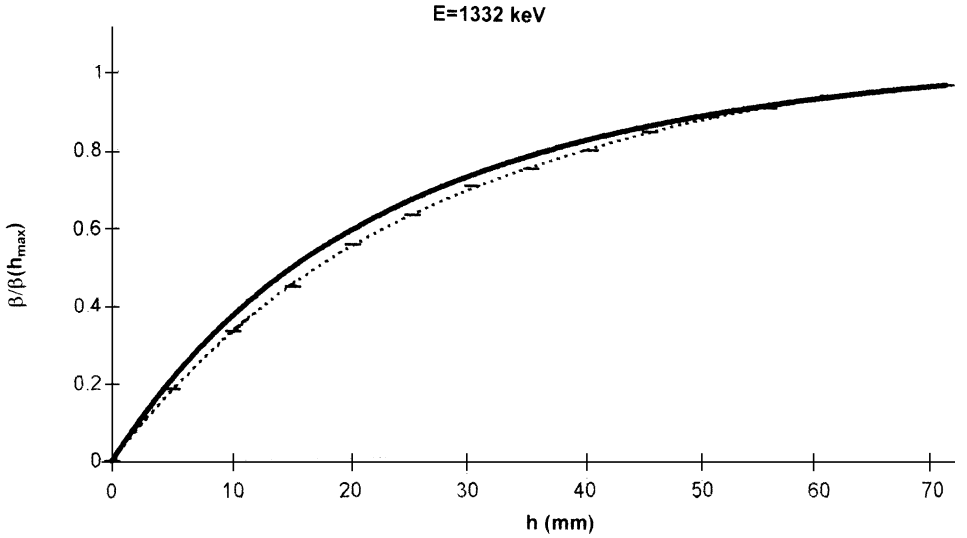

Fig. 13. Normalized β functions, theoretical and experimental, for 1332 keV. The dot lines represent the experimental function.

V	sample-volume
w_k	distance travelled by the kth photon through the detector
x_k	distance travelled by the kth photon through the sample
Y	characteristic gamma-ray yield
β	beta quantity (defined on this work). Photopeak β
β_t	total β
β_{exp}	experimental photopeak β
ε	sample detector system efficiency. Photopeak efficiency
ε_t	sample detector system total efficiency
ε_{int}	intrinsic detector efficiency
ε^S	sample-section detector system efficiency
μ_D	detector attenuation
μ_M	sample attenuation
ρ	sediment density
Ω	solid angle subtended at the sample section by the detector

Acknowledgements

This work has been supported by the II Plan Andaluz de Investigación of the Junta de Andalucía (Spain) and the FEDER program (E.U.).

Appendix A.

The β quantity, defined in Eq. (9), verifies the following properties:

(1) Let us consider a sample–detector system, and we suppose two zones inside the sample, 1 and 2, as it can be seen in Fig. 14. The whole system will have an efficiency, ε, and a volume V. Besides, the radioisotope must be homogenized inside the sample, and we call a to the activity per volume unit. The total number of detections comes from region 1 and 2. We can define an efficiency for every one of these regions, $\varepsilon_i = D_i/N_i$, with N_i the number of emissions in the region i and D_i the number of detections for these emissions. So,

$$N_i = A_i Y t = V_i a Y t, \tag{A.1}$$

where Y is the gamma-ray yield and t is the counting time. So, the number of detections coming from each region can be written like:

$$D_1 = \varepsilon_1 V_1 a Y t, \quad D_2 = \varepsilon_2 V_2 a Y t. \tag{A.2}$$

We can write for the number of detections coming from the whole sample and from each region, the following expressions:

$$D = \beta a Y t, \quad D_1 = \beta_1 a Y t, \quad D_2 = \beta_2 a Y t, \tag{A.3}$$

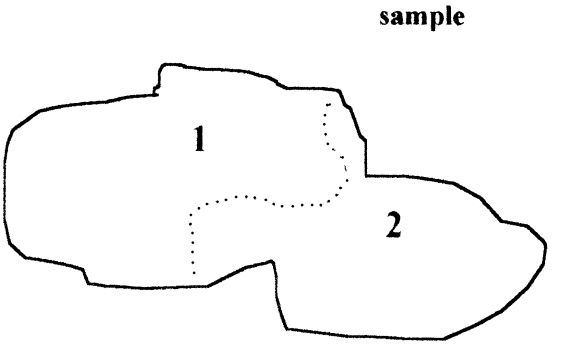

Fig. 14.

where we have used β for the whole sample and β_i for region i. As $D = D_1 + D_2$, we get

$$\beta = \beta_1 + \beta_2. \tag{A.4}$$

This property is not satisfied for the efficiency. From the previous expression, we can get:

$$\varepsilon = \frac{V_1}{V}\varepsilon_1 + \frac{V_2}{V}\varepsilon_2 \tag{A.5}$$

which it shows the non-additive relationship between efficiencies.

Eq. (A.4) is completely general and does not depend on the geometry or the composition of the sample (it can even be heterogeneous). However, we have employed homogeneity of the radionuclide inside the sample.

(2) For cylindrical geometry, $\beta(h)$ is an increasing function and it has a finite limit. So, the following properties are satisfied:

$$\beta(h_1) < \beta(h_2) \quad \text{if} \quad h_1 < h_2, \tag{A.6}$$

$$0 < \beta(\infty) < \infty \quad \text{where} \quad \beta(\infty) = \beta(h \to \infty). \tag{A.7}$$

Property A.6 comes directly from Eq. (A.4). In Fig. 15, we represent the cross-section of a cylindrical sample with two possible heights, h_1 and h_2, which limit the regions 1 and 2. As $\beta(h_1) = \beta_1$ and $\beta(h_2) = \beta_1 + \beta_2$, we have that $\beta(h_1) < \beta(h_2)$, as β quantity is positive.

In order to demonstrate Eq. (A.7), we consider a cylindrical sample in which height h_2 is infinite, as we can see in Fig. 16. As $\beta(h_2) = \beta_1 + \beta_2$, we only have to show that β_2 is finite. For this reason, we

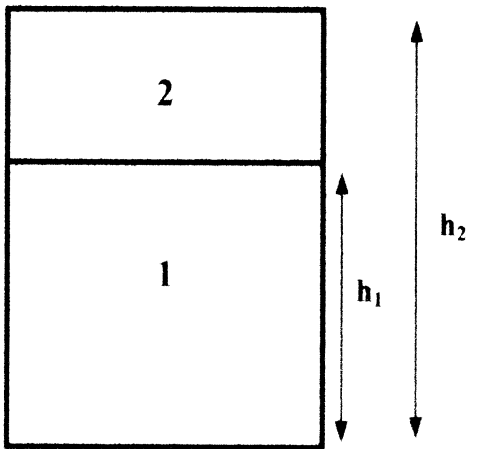

Fig. 15.

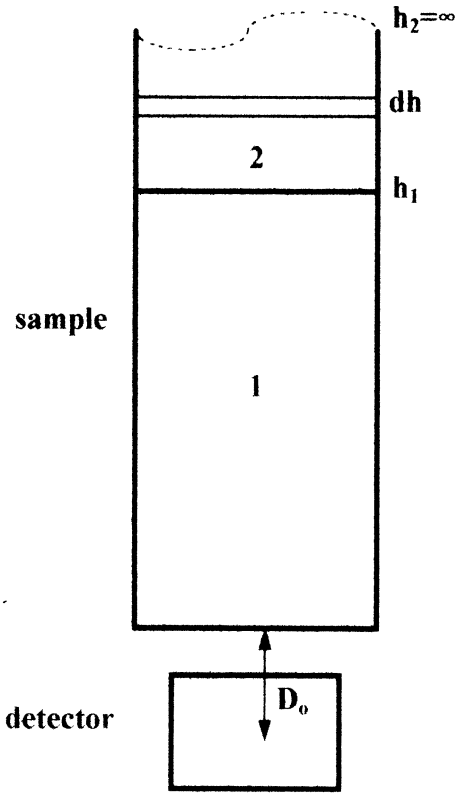

Fig. 16.

consider the differential sections $d\beta$ in region 2, and we write by the additive property of β:

$$\beta_2 = \int_{h=h_1}^{h=\infty} d\beta \tag{A.8}$$

We can write $d\beta$ like:

$$d\beta = \varepsilon^S(h)\, dV = \varepsilon^S(h)\pi R_M^2\, dh \tag{A.9}$$

where $\varepsilon^S(h)$ is the section efficiency, dV is the section volume and R_M is the sample radius. If we choose h_1 large enough, we can write $\varepsilon^S(h)$ like a product of three probabilities, $\varepsilon^S(h) = p_1 p_2 p_3$, where p_1 is the probability for the photon to be emitted from the section toward the detector in the solid angle $\Omega(h)$, $p_1 = \Omega(h)/4\pi$; p_2 is the probability for the photon not to be absorbed in the pathway to the detector, $p_2 = e^{-\mu_M h}$; and p_3 is the probability for the photon to be detected when it crosses the detector, also known as the intrinsic efficiency, $p_3 = \varepsilon_{int}$ which only depends on the detector and the energy of the photon, but not on the sample geometry. For a given section of sample, a πR_D^2 detector surface is seen, where R_D is the detector radius, and $h + D_0$ is the distance from the section to the detector, and D_0 is the distance between the sample-bottom and detector–center (Fig. 16). So,

$$p_1 = \frac{R_D^2}{4(h + D_0)^2} \tag{A.10}$$

and we can write

$$d\beta = \frac{\pi}{4} R_M^2 R_D^2 \varepsilon_{int} \frac{e^{-\mu_M h}}{(h + D_0)^2}\, dh \tag{A.11}$$

So, considering Eq. (A.8), we get

$$\beta_2 = \frac{\pi}{4} R_M^2 R_D^2 \varepsilon_{int} \int_{h=h_1}^{h=\infty} \frac{e^{-\mu_M h}}{(h + D_0)^2}\, dh \tag{A.12}$$

and as the integral in this equation has a finite value, β_2 is also a finite quantity.

References

[1] G. Haase, D. Tait, A. Wiechen, Nucl. Instr. and Meth. A 329 (1993) 483.

[2] G. Haase, D. Tait, A. Wiechen, Nucl. Instr. and Meth. A 361 (1995) 240.

[3] K. Debertin, R.G. Helmer, in: Gamma and X-ray Spectrometry with Semiconductor Detectors, Elsevier, North-Holland, Amsterdam, 1988, p. 342.

[4] N.H. Cutshall, I.L. Larsen, C.R. Olsen, Nucl. Instr. and Meth. B 206 (1983) 309.

[5] M.E. Kitto, Appl. Rad. and Isot. 42 (9) (1991) 961.

[6] J.P. Bolívar, Tesis de licenciatura, Universidad de Sevilla, 1993, (In Spanish).